

WGAN-based Autoencoder Training Over-the-air

Sebastian Dörner, Marcus Henninger, Sebastian Cammerer, and Stephan ten Brink
Institute of Telecommunications, Pfaffenwaldring 47, University of Stuttgart, 70659 Stuttgart, Germany
{doerner,cammerer,tenbrink}@inue.uni-stuttgart.de

Abstract—The practical realization of end-to-end training of communication systems is fundamentally limited by its accessibility of the channel gradient. To overcome this major burden, the idea of generative adversarial networks (GANs) that learn to mimic the actual channel behavior has been recently proposed in the literature. Contrarily to handcrafted *classical* channel modeling, which can never fully capture the real world, GANs promise, in principle, the ability to learn any physical impairment, enabled by the data-driven learning algorithm. In this work, we verify the concept of GAN-based autoencoder training in actual over-the-air (OTA) measurements. To improve training stability, we first extend the concept to conditional Wasserstein GANs and embed it into a state-of-the-art autoencoder-architecture, including bit-wise estimates and an outer channel code. Further, in the same framework, we compare the existing three different training approaches: model-based pre-training with receiver finetuning, reinforcement learning (RL) and GAN-based channel modeling. For this, we show advantages and limitations of GAN-based end-to-end training. In particular, for non-linear effects, it turns out that learning the whole exploration space becomes prohibitively complex. Finally, we show that the training strategy benefits from a simpler (training) data acquisition when compared to RL-based training, which requires continuous transmitter weight updates. This becomes an important practical bottleneck due to limited bandwidth and latency between transmitter and training algorithm that may even operate at physically different locations.

I. INTRODUCTION

Since the first publication of *autoencoder*-based communications [1], the vision of end-to-end training of communication systems has attracted an impressive amount of follow-up work. Thereby, end-to-end learning has found its entry into virtually any field of today’s communications research – in the wireless [2] and optical [3] domain, but also emerging domains, like the molecular [4] channel. Although autoencoder-based communication promises a framework that operates over any channel, for practical deployment the *missing channel gradient* [5] prevents joint end-to-end training of transmitter and receiver.

To overcome this major obstacle of end-to-end training, a model-based pre-training technique has been proposed in [5]. For this, the transceiver is trained end-to-end for a handcrafted channel model and, in a second step, only the receiver is *finetuned* to the actual channel conditions using pilot transmissions without the need of a channel gradient. Obviously, the success of this approach depends on the accuracy of the model; however, it is in the very nature of things that a model never fully captures all real world effects.

A different approach is presented in [6] based on RL techniques and, in particular, policy gradient methods. By adding

artificial perturbation noise to the transmitted message and feeding back the current reward (i.e., the receiver’s estimation accuracy) from the receiver to the transmitter, an estimate of the actual gradient can be obtained. This closed-loop between transmitter and receiver allows end-to-end training without an existing gradient in-between. However, it also requires a continuous feedback link as each gradient update creates a new set of transmitter weights that needs to be deployed.

As an alternative training procedure, GANs [7] have been proposed in [8] to first approximate the channel and, afterwards, train the autoencoder based on the thereby gathered channel model. Or, in other words, the idea of pre-training with an *explicit* model is extended towards an *implicit* channel model stemming from a data-driven training process based on real-world samples. It has been shown in [9], [10] for simulated channels that, in principle, a GAN can *mimic* simple channel models, and autoencoder training is possible. The authors of [3] demonstrate that for optical intensity modulation (IM) and direct detection (DD) receivers, a channel GAN can be learned. However, to the best of our knowledge, this has not been verified in the field by a practical OTA setup for wireless communications yet. Contrary to [9], [10], the wireless channel can become an attractive subject of investigation once multipath and, thus, frequency-selectivity becomes part of the transmission. We utilize the orthogonal frequency division multiplex (OFDM)-autoencoder structure from [11] and optimize the autoencoder for *bit-wise* information transmission as introduced in [12]. Further, we utilize Wasserstein generative adversarial networks (WGANs) [13] for improved convergence and training stability. We aim to provide a comparison with reinforcement learning and model-based pre-training with receiver finetuning in a unified framework.

When it comes to practical implementations, the communication overhead between training algorithm (e.g., local GPU-server or even a remote cloud instance) and transceiver implementation (e.g., software-defined radio (SDR) or field programmable gate array (FPGA)) matters and can become a practical bottleneck of the training procedure. Therefore, we show that training of GANs only requires a single dataset that can be collected in a *one-shot* transmission while this is not possible for RL-based training. Thus, training can be fully done at the receiver and only the updated transmitter weights have to be sent back to the transmitter, while in RL training, a continuous feedback of the reward must be ensured. This can be further combined with online retraining through label-recovery via outer channel codes at the receiver (cf. [14]).

II. STATE OF THE ART AUTOENCODER SYSTEMS

Most of the previously proposed fully end-to-end trained autoencoder-based communication systems rely on optimizing the mutual information between channel input and channel output by minimizing the symbol-wise categorical cross-entropy (CE) (see [12] for a detailed derivation). The big drawback of this symbol-wise architecture is that it cannot be scaled to practical (bit) sequence lengths, as it suffers from the *curse of dimensionality* [15]. Such scaling implies that powerful coding schemes, comparable to state-of-the-art systems, must be *learned* from scratch, which is simply too complex. To reduce this complexity, practical systems usually rely on bit-interleaved coded modulation (BICM) and bit-metric decoding (BMD). We follow the approach of [12] and combine the autoencoder NN in the BICM framework with an outer channel code which can be decoded by a fully differentiable belief propagation (BP) decoder. Such an autoencoder system can then be trained in an end-to-end manner to maximize the bit-wise mutual information (BMI) at its output, which is also the decoder's input, and, thereby, inherently learns the optimal constellation shaping and bit labeling. Throughout this work, we use the bit-wise iterative autoencoder architecture as described in [12] with an outer IEEE 802.11n WLAN irregular low-density parity-check (LDPC) code of rate $r = 1/2$, length $n = 1296$ bit and 40 iterations of iterative demapping and decoding (IDD) between the autoencoder receiver and the differentiable BP decoder.

The whole setup is shown in Fig. 1a; transmitter NN and receiver NN are shown in Fig. 1b and Fig. 1c, respectively. At the transmitter side, an LDPC encoder encodes a bitstream into codewords \mathbf{c} , which are sliced into s bit vectors $\mathbf{b}^{(i)}$, i.e., s autoencoder messages of length m bits, where n is a multiple of m . For simplicity, interleaver and deinterleaver are considered as part of the LDPC graph, and are therefore not shown. The transmitter with trainable weights matrix $\theta_T \in \mathbb{R}^{2^m \times 2}$ then maps each bit vector $\mathbf{b}^{(i)}$ into a symbol $x_i \in \mathbb{C}$, representing one complex baseband channel use, which is then sent over the channel. At the receiver side, the receiver NN with trainable weights θ_R takes, as a concatenated input, the received symbol $y_i \in \mathbb{C}$, a signal-to-noise-ratio (SNR) estimation and *a priori* knowledge provided by the BP decoder in form of m log-likelihood ratios (LLRs) $\mathbf{l}_E^{(i)} \in \mathbb{R}^m$ and outputs m LLRs $\mathbf{l}^{(i)} \in \mathbb{R}^m$. These s LLRs $\mathbf{l}^{(i)}$ are concatenated to a vector \mathbf{l} of length n and forwarded to the BP decoder. For the first iteration it is $\hat{\mathbf{l}}_E = \mathbf{0}$; after 40 iterations of IDD the BP decoder finally outputs the resulting $\hat{\mathbf{l}}$.

A. Training Approaches

As previously mentioned, the idea of this autoencoder setup is to maximize the BMI at the receiver's output, which is shown in [12] to be closely related to minimizing the total binary CE, and leads to the following loss definition¹

¹Note that we define the loss via the expectation operator. However, as usually done in deep learning, the loss is approximated by the mean of randomly drawn samples from a mini-batch.

$$\mathcal{J}(\theta_T, \theta_R) := H(p_{\theta_T}(\mathbf{c}|\mathbf{y}), \tilde{p}_{\theta_R}(\mathbf{c}|\mathbf{y})) \quad (1)$$

$$= \mathbb{E}_{\mathbf{y}, \mathbf{c}} [-\log \tilde{p}_{\theta_R}(\mathbf{c}|\mathbf{y})] \quad (2)$$

where $\tilde{p}_{\theta_R}(\mathbf{c}|\mathbf{y})$ is the posterior distribution obtained by applying the sigmoid function to the logits \mathbf{l} generated by the receiver NN and estimated over a batch of multiple (at least one) LDPC codewords.

In the case of a channel model with known channel gradient, we simply train in an unsupervised end-to-end learning fashion, where both θ_T and θ_R can be updated jointly using stochastic gradient descent (SGD) on loss (2). However, after deployment on an actual channel, the channel gradient is unknown and only θ_R can be updated straightforwardly using backpropagation, described as *finetuning* in [5]. Here, the transmitter generates a batch of symbols \mathbf{x} , which are then sent over the actual channel and the received symbols \mathbf{y} are recorded at the receiver. The receiver weights θ_R can then easily be trained in a supervised fashion using SGD on loss (2), while backpropagation stops at the channel as the recorded symbols \mathbf{y} and the corresponding labels \mathbf{c} are fed.

To be able to operate close to the actual channel capacity, one also needs to optimize the transmitter weights θ_T to shape the optimal constellation. Therefore, we distinguish between two different approaches:

- **RL-based training** as proposed in [6]: transmitter and receiver are trained in an *alternating* fashion. Training of the receiver follows the principle of the previously described receiver finetuning, while training of the transmitter relies on an approximation of the channel's gradient by adding random perturbations \mathbf{w} to the transmitter's output symbols \mathbf{x} during training. If the added perturbation improves the loss at receiver side, the gradient follows the perturbation, as described in [6], and the transmitter can be trained on the loss

$$\hat{\mathcal{J}}(\theta_T) = \mathbb{E}_{\mathbf{y}, \mathbf{c}, \mathbf{w}} [-\log \tilde{p}_{\theta_R}(\mathbf{c}|\mathbf{y})]. \quad (3)$$

On the one hand, this process proved to be quite reliable for suitable hyperparameters (e.g., amount of exploration noise, learning rates, and the ratio between θ_T and θ_R updates). But, on the other hand, as this process depends on slight random explorations, the transmitter weights θ_T must be adjusted after each gradient step.

- **GAN-based training** as first proposed in [8]: the idea is to first train a generator NN to mimic the channel with all its effects, including hardware insufficiencies. Once the generator is able to approximate the channel distribution $p(\mathbf{y}|\mathbf{x})$ satisfactorily, one can use this differentiable generator NN as a channel model for conventional unsupervised autoencoder end-to-end training using SGD on loss (2), see Fig. 1a.

B. Over-the-air Setup

For actual over-the-air measurements, we use a wireless communication system consisting of two universal software radio peripherals (USRPs) B210 from Ettus Research with carrier frequency of $f_c = 2.35$ GHz and an effective bandwidth of

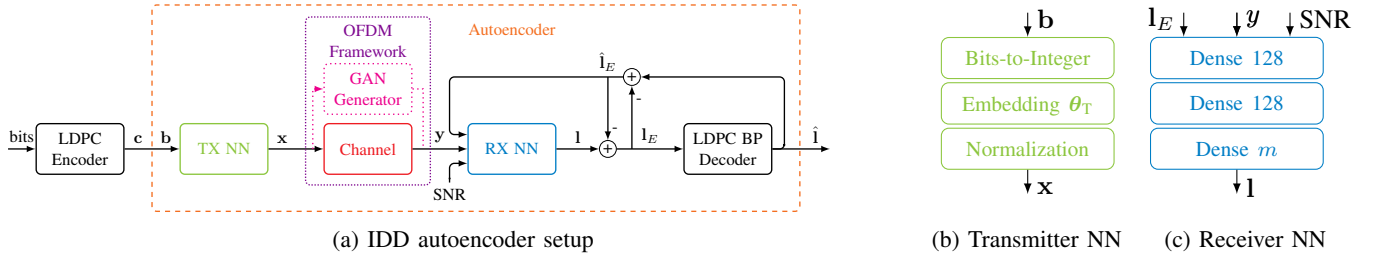


Fig. 1: Bit-wise iterative autoencoder system with transmitter and receiver NN structure. Dense layers are labeled with their number of neurons n_{neurons} . Throughout this work all layers use biases and are ReLU activated, except for output layers.

15.94 MHz in a static indoor office environment. An OFDM-based framework with cyclic prefix (CP) of ratio $1/8$ and 64 subcarriers (50 of which are used for data transmission), as first introduced in [11], was added as a channel interface to the autoencoder architecture shown in Fig. 1a. On the transmitter side, this framework maps the transmitter symbols \mathbf{x} into an OFDM structure, performs an inverse fast Fourier transform (IFFT), and adds the CP before the transmission of $\mathbf{x}_{\text{OFDM}} \in \mathbb{C}$ over the USRP channel. On the receiver side, it synchronizes OFDM symbol transmissions using the CP, performs a fast Fourier transform (FFT), and re-maps all symbols $\mathbf{y}_{\text{OFDM}} \in \mathbb{R}$ back into the expected shape \mathbf{y} of the autoencoder architecture. The CP was only used for synchronization and was not accessible to the NN. Linear minimum mean square error (MMSE) equalization of the received symbols was performed on a per-subcarrier-basis prior to NN-based demapping.² To estimate the SNR required by the demapper, we first calculate the error vector magnitude (EVM) between the originally sent symbols and the equalized received symbols. We then calculate an average SNR per sub-carrier, defined by the mean over the EVM, and feed this SNR estimation to the demapper of the corresponding sub-carrier.

III. GENERATIVE ADVERSARIAL NETWORKS FOR AE TRAINING

GANs consist of two separate adversarial NNs, a generative and a discriminative model, which essentially play a two-player *minimax* game [7]. While the generator G tries to reproduce the underlying data distribution p_r from a latent variable \mathbf{z} (realizing random Gaussian noise) to fool the discriminator D , the discriminator aims to distinguish generated samples $G(\mathbf{z})$ from real samples \mathbf{y} by outputting the estimated probability of the current sample being drawn from the real distribution. As we aim to mimic the channel transition probability $p(\mathbf{y}|\mathbf{x})$, the GAN is implemented as a conditional GAN [16], i.e., conditioned on the transmitted message \mathbf{x} . The resulting value function is given as

$$\min_G \max_D \mathbb{E}_{\mathbf{x}, \mathbf{y} \sim p_r(\mathbf{y})} [\log(D(\mathbf{y}|\mathbf{x}))] + \mathbb{E}_{\mathbf{x}, \mathbf{z} \sim p_z(\mathbf{z})} [\log(1 - D(G(\mathbf{z}|\mathbf{x})|\mathbf{x}))]. \quad (4)$$

²In [11], it has been shown that the autoencoder can learn MMSE equalization, however, this requires multiple complex-valued channel uses. For simplicity and a fair comparison with a quadrature amplitude modulation (QAM)-baseline, this is not considered, yet an extension is straightforward.

Although theoretically very powerful, GANs often suffer from training instability and, hence, require both networks to be synchronized well.

A. Wasserstein GAN

To ensure a more stable training convergence and, in particular, to enable stable training with longer sequences \mathbf{x} and \mathbf{y} , a different loss function can be used. For this, Wasserstein GANs [13] facilitate training by employing the earth mover's distance (EMD) (or Wasserstein-1 distance), which is given as

$$W(p_r, p_g) = \inf_{\gamma \in \Pi(p_r, p_g)} \mathbb{E}_{(x, y) \sim \gamma} [||x - y||] \quad (5)$$

where $\Pi(p_r, p_g)$ is the set of all joint distributions between p_r and p_g . The EMD is merely a different measure of similarity between distributions and can be thought of as the minimum amount of cost when transforming one probability distribution into the other [17]. One particular distribution γ describes this perfect *transport plan*. Under mild assumptions, the EMD is continuous everywhere and differentiable almost everywhere [13] and, therefore, yields more favorable optimization properties than the Jensen-Shannon divergence.

The infimum in Eq. (5) is intractable, but using the Kantorovich-Rubinstein duality the Wasserstein distance can be approximated [13], leading to the following value function

$$\min_G \max_{C \in \xi} = \mathbb{E}_{\mathbf{x}, \mathbf{y} \sim p_r(\mathbf{y})} [C(\mathbf{y}|\mathbf{x})] - \mathbb{E}_{\mathbf{x}, \mathbf{z} \sim p_z(\mathbf{z})} [C(G(\mathbf{z}|\mathbf{x})|\mathbf{x})] \quad (6)$$

where ξ is the set of 1-Lipschitz functions.

D now outputs a score rather than a probability for each sample, which is why it is usually referred to as the critic C within the framework of a WGAN. The loss function of an optimally trained critic provides a reliable approximation of the Wasserstein-1 distance between both distributions. Therefore, the fundamental idea is to train C under the established Lipschitz constraint sufficiently long so that a good enough estimate of the distance can be obtained, which G can then propagate back through to obtain the gradients for updating its weights.

B. Implementation and Training

From Eq. (6), we can straightforwardly infer the loss functions for generator and critic for our task

$$\mathcal{J}_G = -\mathbb{E}[C(\mathbf{y}_g|\mathbf{x})] \quad (7)$$

$$\mathcal{J}_C = \mathbb{E}[C(\mathbf{y}_g|\mathbf{x})] - \mathbb{E}[C(\mathbf{y}_r|\mathbf{x})] + \lambda_{\text{GP}} \mathcal{J}_{\text{GP}} \quad (8)$$

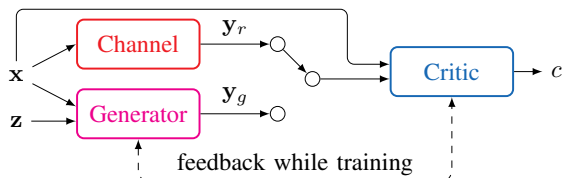


Fig. 2: Conditional WGAN architecture

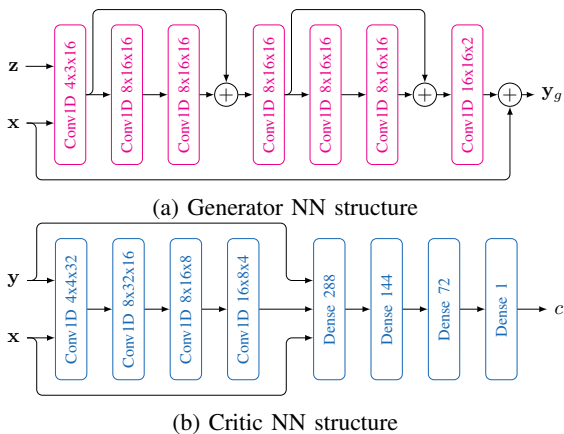


Fig. 3: Layer structures of generator and critic NN. Hyperparameters for CNN layers are given as $\ell_{\text{kernel}} \times n_{\text{channels}} \times n_{\text{filters}}$. where λ_{GP} is a hyperparameter; to enforce the aforementioned Lipschitz constraint, we add a gradient penalty \mathcal{J}_{GP} to the critic's loss function defined as

$$\mathcal{J}_{\text{GP}} = \mathbb{E}[\max\{0, \|\nabla_{\hat{y}} C(\hat{y})\|_2 - 1\}^2] \quad (9)$$

which penalizes C if the gradient norm is strictly greater than one [18].

The generator network is fed the current AE sequence \mathbf{x} as well as normally distributed random noise \mathbf{z} as a condition, while the inputs for the critic are either the generated message y_g or the real one y_r (after being transmitted OTA), along with the respective AE sequence \mathbf{x} . As our setup requires the generator to accurately mimic the channel for at least one OFDM symbol of length $\ell_{\text{OFDM}} = \ell_{\text{sub}} + \ell_{\text{CP}}$ symbols in time domain, both networks are mostly composed of convolutional neural networks (CNNs), allowing the WGAN to scale well to long input sequences. Furthermore, we use shortcut connections (i.e., residual NN structures) to cope with the vanishing gradient problem [19]. The resulting WGAN architecture is depicted in Fig. 2 and the structures of the generator and critic NNs are shown in Fig. 3a and Fig. 3b, respectively.

Training of the WGAN needs to be done in an alternating fashion, where critic and generator weights θ_C and θ_G are updated separately, as their loss functions Eq. (8) and Eq. (7) depend on each other's weights. We used the algorithm shown in Alg. 1, which aims at always improving the weaker player in the minimax game using SGD together with the Adam optimization algorithm.

After training the WGAN sufficiently, the critic may be discarded and the learned generator NN can now be used as the channel model to train the AE, as described in Sec. II-A.

Algorithm 1: WGAN training algorithm

Data: Generated \mathbf{x} and measured y_r

Result: Optimized generator weights θ_G

repeat

draw random batches $\mathbf{x}_b, y_{r,b}$ out of \mathbf{x}, y_r ;

generate $y_{g,b} = G(\mathbf{z}_b|\mathbf{x}_b)$;

if $\mathbb{E}[C(y_{g,b}|\mathbf{x})] < \mathbb{E}[C(y_{r,b}|\mathbf{x}_b)]$ **then**

update θ_G according to Eq. (7);

else

update θ_C according to Eq. (8);

end

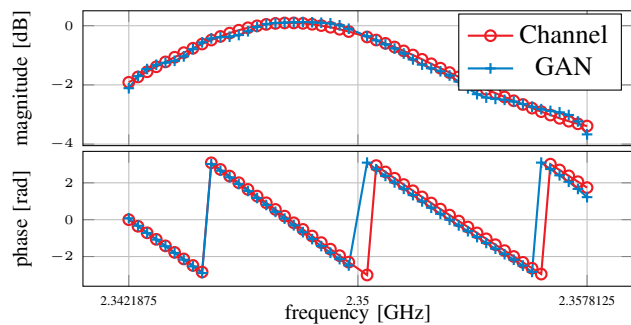


Fig. 4: Measured OTA and generated frequency response in magnitude and phase. Averaged over 259,200 OFDM symbols.

IV. RESULTS

In the following, we present results measured over an actual wireless channel within a static office environment. To graphically demonstrate the generator's performance, Fig. 4 depicts the frequency response for each used sub-carrier in magnitude and phase for the measured OTA channel and the learned generator channel realizations. As can be seen, the WGAN inherently matches the frequency response of the actual measured OTA channel closely, although it has only been trained on time domain sequences. But, to achieve these results, we needed to add a pre-processing step that zero-forces the phase ϕ_0 of the first sub-carrier in time domain, as due to slight carrier frequency offset (CFO) we noticed random ϕ_0 for different measurements. Consistent with observations while using a simulated tapped delay line (TDL) channel model with five random channel taps, the WGAN did not converge due to the generator getting stuck in single modes. We figured that the complexity of the general task of *learning* the convolution operation is too complex for our WGAN setup and, therefore, reduced the task to a static channel, which led to reliable generalization and the WGAN-setup was then able to improve the autoencoder's constellation.

Finally, Fig. 5 shows the bit error rate (BER) performance over the OTA channel for five different setups. The baseline 16-QAM-setup, which uses a conventional demapper with maximum a posteriori (MAP) performance assuming an additive white Gaussian noise (AWGN) channel³, is depicted

³The AWGN MAP demapper is expecting a perfectly Gaussian noise distribution, while in the OTA setup, it is exposed to all channel effects, hardware insufficiencies (like quantization, clipping and non-linear effects), and distortions due to MMSE equalization, which finally lead to a different LLR distribution and, thereby, to non-optimal demapping.

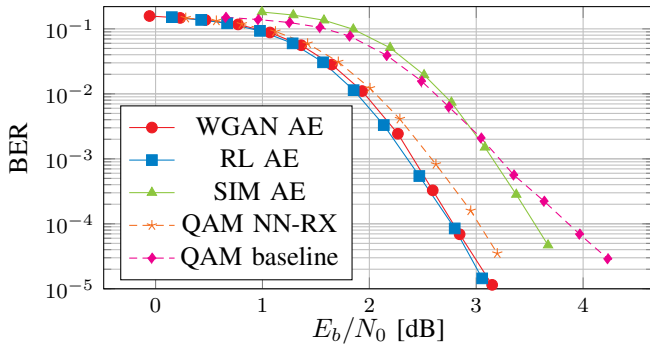


Fig. 5: Final OTA bit error rates after 40 iterations of iterative decoding and demapping using a BP decoder and a standard IEEE 802.11n irregular LDPC code of length $n = 1296$ bits.

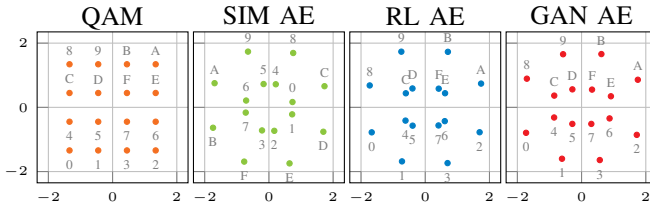


Fig. 6: Used constellations and labels depicted in Hex notation.

as *QAM baseline*. It shows the second worst performance, as it uses a non-optimized constellation on transmitter side and also uses a non-optimal demapper at receiver side. With an up to 1dB better performance, we can see the 16-QAM-setup *QAM NN-RX*, which uses a finetuned NN-based demapper. It still uses a non-optimized QAM constellation, but indicates what can be gained at the receiver side by optimizing an NN-based demapper via finetuning. The remaining BER curves show the performance of learned autoencoder constellations, depicted in Fig. 6. As we can see, the *SIM AE* setup, whose constellation has only been optimized for a simulated random TDL channel model, shows an even worse performance than the *QAM baseline* setup as its constellation and labeling, which easily outperformed the *QAM baseline* over the simulated channel, seem to be counterproductive on the actual OTA channel. This again shows the importance of enabling end-to-end training through the actual channel, as there will always be a mismatch between channel model and actual channel, which, in this case, even resulted in a degraded constellation and labeling. Finally, both end-to-end optimized setups *RL AE* and *WGAN AE* actually improve the BER compared to the QAM constellation by roughly 0.2dB as they were able to optimize the used constellation at transmitter side through the channel. We can see the *RL AE* still performing slightly better than the *WGAN AE*, but the key difference between both setups is that the RL-based setup (with empirically optimized training hyperparameters) required roughly 10,000 transmitter weight updates during training, while the WGAN-based setup was updated offline over the learned WGAN channel and the final transmitter weights θ_T were updated only once. In terms of deployment complexity, the WGAN-setup thereby dramatically reduces transmission and weight update overhead of end-to-end training over the actual channel. One could

further alternate between WGAN and autoencoder training, as it is done in [3], to finally reach the *RL AE* performance.

V. CONCLUSION AND OUTLOOK

We demonstrated the practicability of WGAN-based autoencoder training by OTA results and shows competitive results when compared to the RL-based training approach [6]. However, it turned out that GANs benefits from a simpler data acquisition as the whole training set can be collected *one-shot* for constant transmitter weights (or at least a much smaller number of iterations). Further, we have also discovered limitations of the WGAN-based training; this is mostly limited by non-stationary channels, i.e., the inability to converge for highly random or dynamic channels, which we consider as key subject of possible future work.

REFERENCES

- [1] T. O'Shea, K. Karra, and T. Clancy, "Learning to communicate: Channel auto-encoders, domain specific regularizers, and attention," in *IEEE Int. Symp. Signal Process. and Inform. Technol.*, 2016, pp. 223–228.
- [2] T. O'Shea and J. Hoydis, "An Introduction to Deep Learning for the Physical Layer," *IEEE Trans. Cogn. Commun. Netw.*, vol. 3, no. 4, pp. 563–575, Dec. 2017.
- [3] B. Karanov, M. Chagnon, V. Aref, D. Lavery, P. Bayvel, and L. Schmalen, "Concept and experimental demonstration of optical im/dd end-to-end system optimization using a generative model," *arXiv preprint arXiv:1912.05146*, 2019.
- [4] N. Farsad and A. Goldsmith, "Neural network detection of data sequences in communication systems," *IEEE Trans. on Signal Process.*, vol. 66, no. 21, pp. 5663–5678, 2018.
- [5] S. Dörner, S. Cammerer, J. Hoydis, and S. ten Brink, "Deep learning based communication over the air," *IEEE J. Sel. Topics in Signal Process.*, vol. 12, no. 1, pp. 132–143, Feb 2018.
- [6] F. Ait Aoudia and J. Hoydis, "Model-free training of end-to-end communication systems," *IEEE J. Sel. Areas Commun.*, vol. 37, no. 11, pp. 2503–2516, Nov 2019.
- [7] I. Goodfellow et al., "Generative adversarial nets," in *Advances in neural information processing systems*, 2014, pp. 2672–2680.
- [8] T. O'Shea, T. Roy, N. West, and B. C. Hilburn, "Physical layer communications system design over-the-air using adversarial networks," in *IEEE EUSIPCO*, 2018, pp. 529–532.
- [9] T. O'Shea, T. Roy, and N. West, "Approximating the void: Learning stochastic channel models from observation with variational generative adversarial networks," in *IEEE ICNC*, 2019, pp. 681–686.
- [10] H. Ye, G. Y. Li, B.-H. F. Juang, and K. Sivanesan, "Channel agnostic end-to-end learning based communication systems with conditional gan," in *IEEE Globecom Workshops*, 2018, pp. 1–5.
- [11] A. Felix, S. Cammerer, S. Dörner, J. Hoydis, and S. ten Brink, "OFDM-autoencoder for end-to-end learning of communications systems," in *IEEE SPAWC*, 2018, pp. 1–5.
- [12] S. Cammerer, F. A. Aoudia, S. Dörner, M. Stark, J. Hoydis, and S. ten Brink, "Trainable communication systems: Concepts and prototype," *arXiv:1911.13055*, 2019.
- [13] M. Arjovsky, S. Chintala, and L. Bottou, "Wasserstein generative adversarial networks," in *Int. Conf. on Machine Learning*, 2017, pp. 214–223.
- [14] S. Schibisch, S. Cammerer, S. Dörner, J. Hoydis, and S. ten Brink, "Online label recovery for deep learning-based communication through error correcting codes," in *IEEE ISWCS*, 2018, pp. 1–5.
- [15] X.-A. Wang and S. B. Wicker, "An artificial neural net Viterbi decoder," *IEEE Trans. Commun.*, vol. 44, no. 2, pp. 165–171, 1996.
- [16] M. Mirza and S. Osindero, "Conditional generative adversarial nets," *arXiv:1411.1784*, 2014.
- [17] Y. Rubner, C. Tomasi, and L. J. Guibas, "The earth mover's distance as a metric for image retrieval," *Int. J. Comput. Vision*, vol. 40, no. 2, pp. 99–121, 2000.
- [18] H. Petzka, A. Fischer, and D. Lukovnikov, "On the regularization of Wasserstein GANs," in *Int. Conf. Learning Representations*, 2018.
- [19] K. He, X. Zhang, S. Ren, and J. Sun, "Deep residual learning for image recognition," *arXiv:1512.03385*, Dec. 2015.